

## ORIGINAL ARTICLES

### Synthesis and Electrical Properties of Polyaniline - Fe<sub>3</sub>O<sub>4</sub> Nanocomposite

<sup>1</sup>Safaa K. El-Mahy, <sup>2</sup>M. Dawy and <sup>3</sup>E.Abd El Aziz

<sup>1</sup>Department of physics, Faculty of Girls for Arts, Science and Education, Ain Shams University, Cairo, Egypt.

<sup>2</sup>Department of Physical Chemistry, National Research Center, Giza, 12622, Egypt.

<sup>3</sup>Department of Inorganic Chemistry, National Research Center, Giza, 12622, Egypt.

---

#### ABSTRACT

Fe<sub>3</sub>O<sub>4</sub> nanoparticle powder were synthesized by a chemical process. Polyaniline – Fe<sub>3</sub>O<sub>4</sub> nanocomposite (PANI-Fe<sub>3</sub>O<sub>4</sub>) were synthesized by a self - assembly method of Fe<sub>3</sub>O<sub>4</sub> nanoparticles with polyaniline. Characterization of the chemical structure of Fe<sub>3</sub>O<sub>4</sub> nanoparticle and its composite using FT-IR and XRD techniques which confirmed the formation of Fe<sub>3</sub>O<sub>4</sub> (maghemite) and Quinoid structure for PANI. Analysis by SEM and TEM were carried out to study the morphology and particle size . PANI consists of long fibrils while the Fe<sub>3</sub>O<sub>4</sub> powder consists of granular particles. Electrical properties of the nanocomposite were studied by measuring the dielectric properties and electrical conductivity in the frequency range 100Hz-5MHz .The conductivity of the nanocomposite linearly increases from 1x10<sup>-5</sup> to 1x10<sup>-2</sup> S/cm. The variation of conductivity with frequency reveals that the charge transport mechanism can be considered to be semiconductor.

**Key words:** Polyaniline; Fe<sub>3</sub>O<sub>4</sub> nanoparticles ; Nanocomposite; Dielectric constant. Ac conductivity

---

#### Introduction

Polyaniline (PANI) is probably the most widely studied due to its several unique properties (Li *et al.* 2007 and Mathur *et al.* 2001). Its ease of preparation, light weight, low cost, better electronic, optical properties, highly stable in air and soluble in various solvents, and good processibility (Li *et al.* 2008; MacDiarmid and Epstein, 1995; Apesteguy and Jacobo, 2004). On the other hand it can be used in many applications, such as electromagnetic interference (EMI) shielding, electro-catalysts, rechargeable battery, light-emitting diodes (LEDs), chemical sensor, biosensor, corrosion devices and microwave absorption (Moghaddam and Nazari, 2008; Sarac *et al.* 2008). Polyaniline (PANI) is one of the most studied conductive polymers due to its easy synthesis, environmental stability, simple doping/dedoping and high conductivity (Chiang and MacDiarmid, 1986; Stejskal and Gilbert, 2002). PANI combined with different NPs to form the nanocomposite has great potential applications such as radar-absorber (Makeiff and Huber 2006), indicators (Drelinkiewicz *et al.* 2007), electrochemical and capacitors (Sun *et al.* 2008), bioelectronic components (Willner *et al.* 2007), catalysts (Amaya *et al.* 2008), gas separation membrane (Weng *et al.* 2011), corrosion inhibitor (Berhard W. 1994), antistatic (Soto-Oviedo *et al.* 2006) and semiconductors (Godovsky *et al.* 2001). One of the promising alternatives to improve the compatibility between Fe<sub>3</sub>O<sub>4</sub> and the matrices Polyurethane (PU) is by modifying the surface of the Fe<sub>3</sub>O<sub>4</sub>. Several deposition methods had been used including electrochemical and chemical deposition of conducting polymer. Electrochemical deposition is not widely used due to difficulty to control the uniform thickening of the polymer over the Fe<sub>3</sub>O<sub>4</sub>. Therefore, chemical deposition of conducting polymer such as polyaniline is selected for surface treatment of Fe<sub>3</sub>O<sub>4</sub> by using in-situ chemical polymerization method, which can overcome the weakness of the previous method (Kazantseva *et al.* 2004). Polyaniline (PANI) having both electrical and magnetic characteristics has been intensively investigated because of its potential applications in electrical, magnetic and electronic devices. Due to some significant characteristics such as very light weight, flexibility and reasonably facile processibility, PANI have recently attracted much interest as electromagnetic interference shielding materials and broad band microwave adsorbing materials (Chandrasekhar and Naishadham 1996 ; Roselena and Inacio 2002). The PANI composites containing Fe<sub>3</sub>O<sub>4</sub> nanoparticles are mostly studied as the PANI having both electrical and magnetic characteristics. Wan's group prepared the PANI nanocomposite containing Fe<sub>3</sub>O<sub>4</sub> nanoparticles using chemical synthesis methods (Wan *et al.* 1996; Wan and Li, 1999; Zhang and Wan, 2003). They found that the nanocomposites had a conductivity from 10<sup>-1</sup> to 10<sup>-4</sup> S/cm, a saturation magnetization of 2–20 emu/g and a coercivity to be about zero. (Deng *et al.* 2002 ; Deng *et al.* 2003) prepared Fe<sub>3</sub>O<sub>4</sub>-PANI nanoparticles with core-shell structure by in situ polymerization. The Fe<sub>3</sub>O<sub>4</sub>-PANI nanoparticles had a conductivity from 1.5×10<sup>-4</sup> to 9.2×10<sup>-5</sup> S/cm, a saturation magnetization of 4.2–48.4 emu/g and a coercivity of 2.0–55.3 Oe. (Apesteguy and Jacobo 2004) obtained Fe<sub>3</sub>O<sub>4</sub>-PANI nanocomposite by using a

chemical method. The Fe<sub>3</sub>O<sub>4</sub>-PANI nanocomposite had a higher saturation magnetization of 72 emu/g and a moderate conductivity of 10<sup>-4</sup> S/cm. According to the results reported (Wan *et al.* 1996; Wan and Li 1999; Zhang and Wan, 2003; Deng *et al.* 2002; Deng *et al.* 2003; Apesteguy and Jacobo 2004), structural, electrical and magnetic properties of the PANI composites containing Fe<sub>3</sub>O<sub>4</sub> nanoparticles were a function of Fe<sub>3</sub>O<sub>4</sub> content and were related to the synthetic method. As is well known, the inorganic-organic nanocomposite containing different inorganic nanomaterials can also be obtained by using a mechanical mixing method. The mechanical mixing method is one of the simplest method to prepare the nanocomposite. Besides this, it is considered that PANI composites, which are formed by using differently doped PANIs, can be used as some functional materials. Various synthetic methods have been reported for obtaining magnetic Fe<sub>3</sub>O<sub>4</sub>-PANI nanocomposite, which include direct precipitation of iron salt in a solution of polymer, oxidative chemical polymerization, the in situ synthesis of polymer via an oxidative or electrochemical procedure in presence of well-dispersed magnetic nanoparticles (Bai and Shi, 2007; Zhang and Wan, 2003). UV-Vis spectroscopy is one of the mostly adopted techniques in characterizing the structures of intrinsically conductive polymers (ICPs), such as polypyrrole (Kim *et al.* 1995; Rajagopalan and Iroh 2002), Polyaniline (PANI) (Albuquerque *et al.* 2000; Malinauskas and Holze 1999; Pruneanu *et al.* 1999), for its convenience (Albuquerque *et al.* 2000; Alexandre and Dubois, 2000), as compared with X-ray photoelectron spectroscopy (Lankri *et al.* 2002; Feng *et al.* 2001 and Chen *et al.* 2001), etc. UV-Vis Absorption spectroscopy measures the percentage of radiation that is absorbed at each wavelength. Typically this is done by scanning the wavelength range and recording the absorbance. UV-Vis absorption spectroscopy is widely used in organic chemistry to investigate the extent of multiple bond or aromatic conjugation within molecules. Vis range and solutions can be easily prepared for many organic compounds.

In the present work, a facile one-step in-situ polymerization method is described to synthesize PANI-Fe<sub>3</sub>O<sub>4</sub> nanostructures using ammonium persulfate (APS) as an oxidant via self-assembly method without the aid of organic dopants or surfactants. The resulting nanocomposite will be analyzed by TEM, SEM, XRD, FT-IR and UV-Vis. AC-conductivity, as well as Dielectric constant will be also studied as a function of frequency range (100Hz-5MHz).

#### *Experimental:*

##### *1. Materials:*

Aniline monomer was distilled twice under reduced pressure before use. The other reagents such as ammonium persulfate (APS, (NH<sub>4</sub>)<sub>2</sub>S<sub>2</sub>O<sub>8</sub>), Aniline (C<sub>6</sub>H<sub>7</sub>N), and p-toluene sulfonic acid (PTSA, C<sub>7</sub>H<sub>8</sub>O<sub>3</sub>S) are purchased from Sigma Aldrich. All the chemicals were used as-received without any further treatment.

##### *2. Synthesis of Fe<sub>3</sub>O<sub>4</sub> nanoparticles:*

Fe<sub>3</sub>O<sub>4</sub> nanoparticles were synthesized according to the following procedures: 0.99 g of ferrous chloride (FeCl<sub>2</sub>.4H<sub>2</sub>O)(5mmol) in 5ml of deionized water and 1.63 g of ferric chloride (FeCl<sub>3</sub>.6H<sub>2</sub>O)(6mmol) in 5ml of deionized water were mixed at room temperature. The above mixture was dropped into 200 ml aqueous ammonia solution (0.6M) in 20 min with vigorous stirring. The pH values of the reaction mixture were kept in the range of 11-12 with the addition of a concentrated ammonium hydroxide solution. The resulting nanoparticles were separated by centrifugation at 2800 rpm for 10 min. The product was washed with distilled water three times and then further washed with ethanol (C<sub>2</sub>H<sub>5</sub>OH) three times and dried in air.

##### *3. Synthesis of PANI-Fe<sub>3</sub>O<sub>4</sub> nanocomposite:*

PANI-Fe<sub>3</sub>O<sub>4</sub> nanocomposite were synthesized via self-assembly method using ammonium persulfate (APS) as an oxidant without the aid of organic dopants or surfactants. The synthesis process is as followed: 0.64 mol/L aniline monomer into polymerization vessel containing 1g. Fe<sub>3</sub>O<sub>4</sub> in 100 ml of 1.14 mol / L H<sub>2</sub>SO<sub>4</sub> acid solution at room temperature and magnetic stirring for 1h. Then 50 ml (1 M) of ammonium persulfate (NH<sub>4</sub>)<sub>2</sub>S<sub>2</sub>O<sub>8</sub> was added to the above mixture reaction. Resulting precipitate was collected by filtration then washed with deionized water and methanol three times respectively. The product was dried in oven at 70°C for 24h to obtain green-black powder of PANI - Fe<sub>3</sub>O<sub>4</sub> nanocomposite.

##### *4. Structural characterization and measurements:*

The as-prepared samples were characterized by X-ray diffraction using (Philips PW 1370) X-Ray diffractometer with Cu, K $\alpha$ , ( $\lambda$  = 0.154 nm), Both transmission electron microscope (TEM, JEOL JEM-3010, 300 kv) and scanning electron microscope (SEM, JEOL JXA -840, Electronic Company, Japan) were used to

characterize the dispersion of  $\text{Fe}_3\text{O}_4$  NPs and the morphology of the PANI-  $\text{Fe}_3\text{O}_4$  nanocomposite. The samples for TEM were prepared by making suspension from the powder in deionized water, A drop of the suspension was put onto the carbon gride and left to dry. The chemical structures of the PANI-  $\text{Fe}_3\text{O}_4$  nanocomposite are characterized by Fourier transform infrared (FT-IR) spectroscopy using (Thermo Nicolet, FT-IR and NEXUS) in the range of  $4000 - 400 \text{ cm}^{-1}$ . UV-Vis spectra of PANI,  $\text{Fe}_3\text{O}_4$  and PANI- $\text{Fe}_3\text{O}_4$  nanocomposite solutions, were measured using (PG Instruments Ltd, T80+UV/Vis, USA spectrometer). The electrical properties at room temperature was measured by (Hioki, LCR Hitester 3532-50). The frequency dependence of electrical properties for as-prepared samples were measured in the frequency range (100 Hz – 5 MHz).

## Results And Discussion

### 1-XRD:

The structure of the PANI,  $\text{Fe}_3\text{O}_4$  and PANI- $\text{Fe}_3\text{O}_4$  powder were confirmed by X-ray diffraction (XRD) as shown in Fig. 1. The XRD patterns of  $\text{Fe}_3\text{O}_4$  are nearly amorphous shape. Fig. 1 reveal that XRD peaks for PANI-  $\text{Fe}_3\text{O}_4$  composite are mostly similar to that of free PANI. XRD spectra of PANI-  $\text{Fe}_3\text{O}_4$  nanocomposite show the diffraction peaks of 26.62 (220), 35.02 (311), 44.02 (4 0 0), 55.80 (511) and 64.05 (4 4 0) (Elsayed *et al.* 2011). Also, It can be noticed that, the structure contains crystalline grains embedded in amorphous matrix. The crystallite size of nanoparticles was calculated using Scherrer's Eq. (1) (Klug and Alexander, 1954):

$$D = \frac{0.9\lambda}{\beta \cos \theta} \quad (1)$$

Where  $D$  is the mean crystallite size (nm),  $\lambda$  is the wavelength of Cu K (0.154 nm),  $\beta$  is the full width at half maximum intensity (FWHM) in radian and  $\theta$  is the Bragg angle in degree (Hua *et al.* 2008 and Chakrabarti *et al.* 2004). The calculations reveal that the average crystallite size of the PANI and  $\text{Fe}_3\text{O}_4$  NPs are about 10.89 and 12.80 nm respectively. Similar results are obtained in the nanocomposite, which is about 13.40 nm. It means that the  $\text{Fe}_3\text{O}_4$  in the PANI- $\text{Fe}_3\text{O}_4$  powder has nanoparticles size. Scherrer formula indicated that there was conglomeration of PANI as coating material for the nanosized  $\text{Fe}_3\text{O}_4$  powder. These results are of much interest, because the more highly ordered systems could display a metallic-like conductive state.

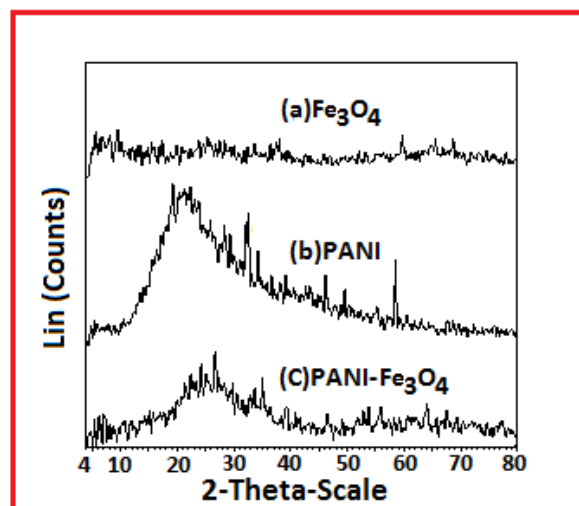


**Fig. 1:** The XRD patterns of (a)  $\text{Fe}_3\text{O}_4$  (b) PANI and (c) PANI-  $\text{Fe}_3\text{O}_4$  nanocomposite.

### 2. SEM:

Fig. 2 shows SEM microphotographs of (a) PANI pellet, (b)  $\text{Fe}_3\text{O}_4$  powder, (c) PANI-  $\text{Fe}_3\text{O}_4$  nanocomposite. As can be seen from Fig. 2, PANI pellet consists of long fibrils while the PANI- $\text{Fe}_3\text{O}_4$  consists of granular particles. Thus, the PANI- $\text{Fe}_3\text{O}_4$  nanocomposite consists of long fibrils and granular particles. It is considered that the partial separation between the  $\text{Fe}_3\text{O}_4$  nanoparticles exists in each pellet.

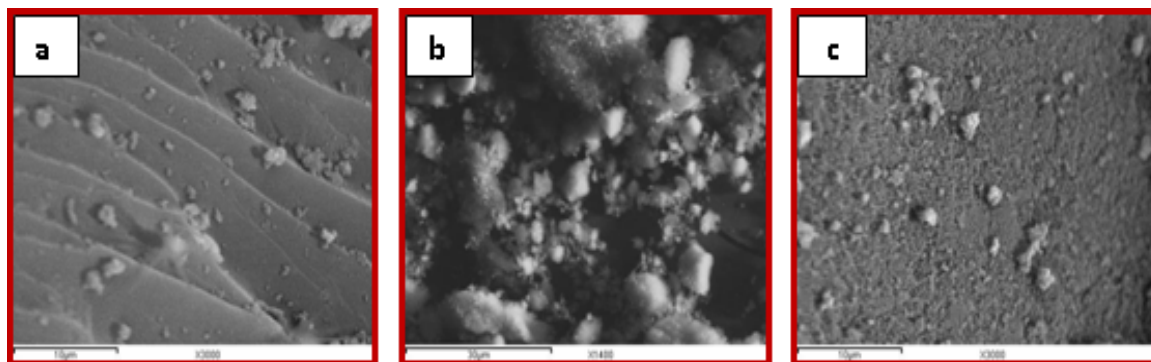


**Fig. 2:** SEM microphotographs of (a) PANI (b)  $\text{Fe}_3\text{O}_4$  (c) PANI-  $\text{Fe}_3\text{O}_4$  nanocomposite.

### 3. TEM:

The TEM images of  $\text{Fe}_3\text{O}_4$  nanoparticles and PANI -  $\text{Fe}_3\text{O}_4$  nanocomposite are shown in Fig.3 (a) and (b) respectively. As shown in Fig.3(a), pure  $\text{Fe}_3\text{O}_4$  nanoparticles look spherical with an average diameter of about 37 nm. Fig.3 (b) indicates that all  $\text{Fe}_3\text{O}_4$  nanoparticles are covered by PANI in nanocomposite.  $\text{Fe}_3\text{O}_4$  nanoparticles encapsulated by PANI are also spherical with an average size of about 46 nm, which is similar to the pure  $\text{Fe}_3\text{O}_4$  nanoparticles shown in Fig.3(a). The interaction between  $\text{Fe}_3\text{O}_4$  nanoparticles and PANI has a positive effect which playing important role on the encapsulation and coating of  $\text{Fe}_3\text{O}_4$  by PANI.

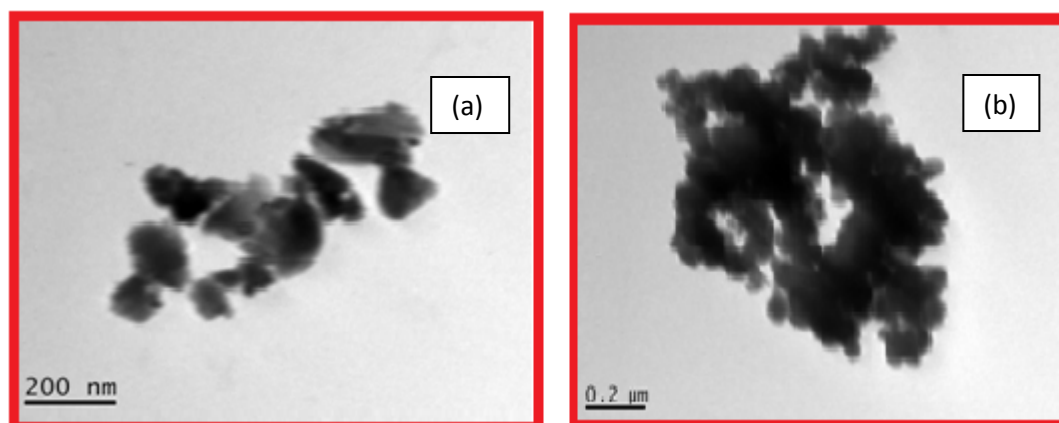
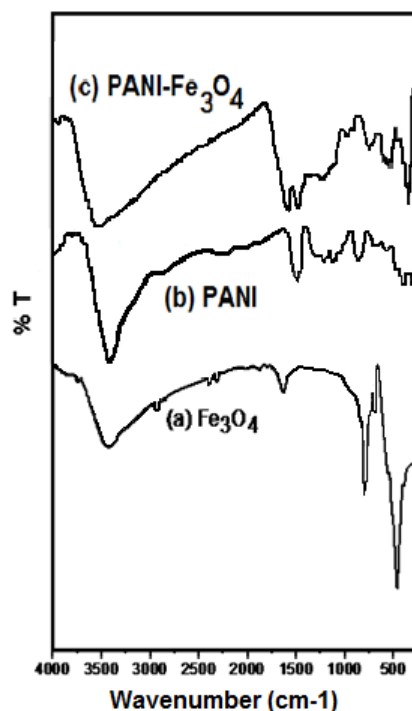


**Fig. 3:** TEM images of (a)  $\text{Fe}_3\text{O}_4$  and (b) PANI- $\text{Fe}_3\text{O}_4$  nanocomposite.

### 4. FT-IR:

The FT-IR spectra were used to determine the chemical structure of the samples. Fig.4. Shows the FT-IR characteristic peaks of (a)  $\text{Fe}_3\text{O}_4$ , (b) PANI and (C) PANI- $\text{Fe}_3\text{O}_4$  nanocomposite. The FT-IR spectrum of  $\text{Fe}_3\text{O}_4$  shows a peak at  $3422\text{ cm}^{-1}$ , which can be assigned to the O-H stretching vibrations in physically adsorbed hydrogen bonded water molecule. The small peak in  $1630\text{ cm}^{-1}$  can also be correlated to the different modes of bonded water molecules existing in the ferrofluid while the prominent peaks at  $458$  and  $696\text{ cm}^{-1}$ , are attributed to the stretching and torsional vibration modes of the Fe-O bonds in tetrahedral and octahedral sites, respectively (Diaz *et al.* 2004). Also, the FT-IR spectrum of PANI shows characteristic peaks at  $3437\text{ cm}^{-1}$  of O-H stretching vibration and  $3100\text{ cm}^{-1}$  assigned to N-H stretching vibrations of amino groups, which are indicative of -NH<sub>2</sub> groups in the structural units of the PANI. The bands at about  $1604$  and  $1350\text{ cm}^{-1}$  arise because of quinoid rings and benzenoid ring units. The presence of these bands clearly indicates that the PANI is composed of both amine and the imine units. The observed band at  $1388\text{ cm}^{-1}$  is ascribed to stretching frequency of B-N = Q moiety (where B refers to benzenoid phenyl rings and Q refers to quinoid phenyl ring) of the PANI-  $\text{Fe}_3\text{O}_4$  nanocomposite. The above spectroscopic data clearly confirms that ferric ion is coordinated with the nitrogen atom of quinoid rings of PANI (Waldron, 1955 and Wan, 1989). The spectrum of the nanocomposite is compared with that of the free PANI. It can be noticed that, important differences in peak positions suggest that some reactions take place on the surface of nanoparticles. For PANI and PANI-  $\text{Fe}_3\text{O}_4$

nanocomposite the bands at 828 and 827  $\text{cm}^{-1}$  respectively are due to C-H out of plane but the peak appeared at 649  $\text{cm}^{-1}$  in the nanocomposite is due to Fe-O stretching band of  $\text{Fe}_3\text{O}_4$  (Alam *et al.* 2007; Bao and Jiang, 2005; Cao *et al.* 2008; Yu *et al.* 2008 ; Kryszewski and Jeszka, 1998) .The noticed shift on the bands at 483 and 549  $\text{cm}^{-1}$  confirmed the introduction of  $\text{Fe}_3\text{O}_4$  in PANI.



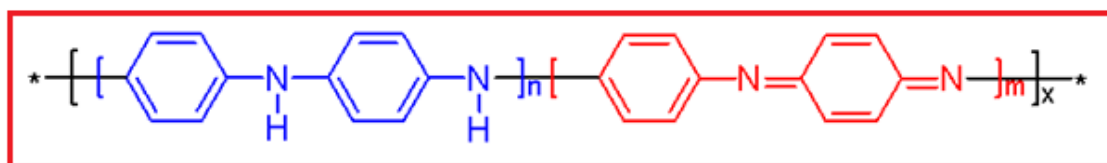
**Fig. 4:** FT-IR spectra of (a)  $\text{Fe}_3\text{O}_4$  , (b) PANI and (c) PANI- $\text{Fe}_3\text{O}_4$  nanocomposite.

Table 1, summarized the main wavenumbers and assignments of the detected active IR-bands for  $\text{Fe}_3\text{O}_4$  , PANI and PANI-  $\text{Fe}_3\text{O}_4$  nanocomposite .

**Table 1:** Comparison between the observed absorption bands of free  $\text{Fe}_3\text{O}_4$  , PANI and PANI- $\text{Fe}_3\text{O}_4$  nanocomposite.

Assignment	Wave number(cm-1)for $\text{Fe}_3\text{O}_4$	Wave number(cm-1)for PANI	Wave number(cm-1)for PANI- $\text{Fe}_3\text{O}_4$ nanocomposite.
O-H stretching vibrations	3422	3437	3379
N-H stretching vibrations of amino groups	—	2930	—
Bonded water molecule	1630	—	—
C=N stretching modes of vibration from quinonoid (NH-Q-NH)	—	1604	1601
C=C stretching modes of vibration from benzenoid unit(NH-B-NH)	—	—	1504
Stretching frequency of B-N = Q moiety	—	—	1388
C-N stretching mode of benzenoid unit	—	1350 and 1265	1342 and 1284
C-H out-of-plane	—	828	827
stretching and torsional vibration modes of the Fe-O bonds	796	-----	649
Fe-O vibrations of Tetrahedral sites	458	-----	483
Fe-O vibrations of octahedral sites	696	-----	549

On comparing assignment of PANI with PANI -Fe<sub>3</sub>O<sub>4</sub> nanocomposite, it can be noticed that, nanocomposite has higher ratio of benzenoid structure, which can affect its electrical and optical properties. Polymerized from the inexpensive aniline monomer, polyaniline can be found in one of three idealized oxidation states: leucoemeraldine – white/clear & colorless (C<sub>6</sub>H<sub>4</sub>NH)<sub>n</sub>, emeraldine – green for the emeraldine salt, blue for the emeraldine base ({[C<sub>6</sub>H<sub>4</sub>NH]<sub>2</sub>[C<sub>6</sub>H<sub>4</sub>N]<sub>2</sub>)<sub>n</sub>) and (per) nigraniline – blue/violet (C<sub>6</sub>H<sub>4</sub>N)<sub>n</sub> (Feast W. J. *et al.* 1996). Fig.5 illustrates main polyaniline structure, where  $x$  equals half the degree of polymerization (DP). Leucoemeraldine with  $n = 1$ ,  $m = 0$  is the fully reduced state. Pernigraniline is the fully oxidized state ( $n = 0$ ,  $m = 1$ ) with imine links instead of amine links. Studies have shown that most forms of polyaniline are one of the three states or physical mixtures of these components. The prepared samples have green colour characterized of emeraldine salt. The emeraldine ( $n = m = 0.5$ ) form of polyaniline, often referred to as emeraldine base (EB), is neutral, if doped or protonated, it is called emeraldine salt (ES), with the imine nitrogens protonated by an acid. Protonation helps to delocalize the otherwise trapped diiminoquinone -diaminobenzene state. Emeraldine base is regarded as the most useful form of polyaniline due to its high stability at room temperature and the fact that, upon doping with acid, the resulting emeraldine salt form of polyaniline is highly electrically conducting. (Alan G. MacDiarmid 2001).



**Fig. 5:** Main polyaniline structures  $n+m = 1$ ,  $x =$  degree of polymerization

The colour change associated with polyaniline in different oxidation states can be used in sensors and electrochromic devices (Huang, *et al.* 2006). Although color is useful, the best method for making a polyaniline sensor is arguably to take advantage of the dramatic changes in electrical conductivity between the different oxidation states or doping levels (Shabnam *et al.* 2004). Treatment of emeraldine with acids increases the electrical conductivity by ten orders of magnitude. The same material can be prepared by oxidation of leucoemeraldine.

##### 5. UV-Vis:

Fig.6. shows UV-Vis spectra of PANI, Fe<sub>3</sub>O<sub>4</sub> and PANI - Fe<sub>3</sub>O<sub>4</sub>. It can be seen from this figure that, there are two characteristic peaks, one at 270 nm and other at 350 nm. The former arises due to  $\pi \rightarrow \pi^*$  transitions, while the latter is due to transition of inter chain charge transfer from two adjacent benzenoid rings to the quinoid ring of PANI chain.

Red shift of both absorption bands as compared to those of pure PANI indicates some type of interaction between Ferric ions with nitrogen atom of PANI. Besides these two peaks, there is a small shoulder peak at 400 nm. This band can be attributed to the charge transfer from nitrogen to the metal center as a result of introducing Iron Oxide particle in PANI. The band gap calculated are 2.19, 2.21 and 2.25 eV for PAN, Fe<sub>3</sub>O<sub>4</sub> and PANI - Fe<sub>3</sub>O<sub>4</sub> respectively.

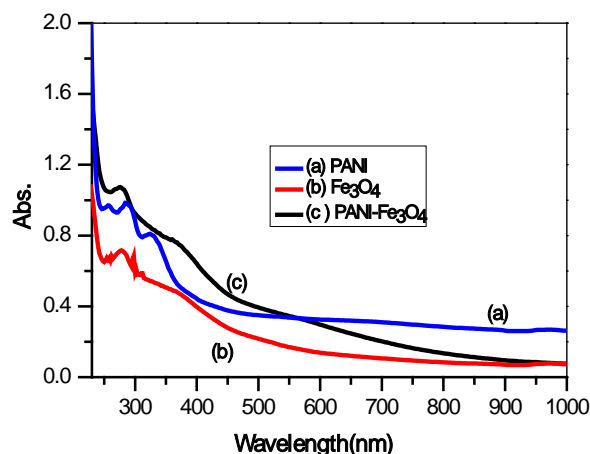


**Fig. 6:** shows UV-Vis spectra of (a)PANI, (b)Fe<sub>3</sub>O<sub>4</sub> and (c) PANI -Fe<sub>3</sub>O<sub>4</sub> nanocomposite solutions.

### 6. Electrical Properties:

AC-conductivity  $\sigma_{a.c.}(\omega)$  of  $\text{Fe}_3\text{O}_4$  and PANI- $\text{Fe}_3\text{O}_4$  nanocomposite have been measured in the frequency range (100Hz-5MHz) at room temperature.

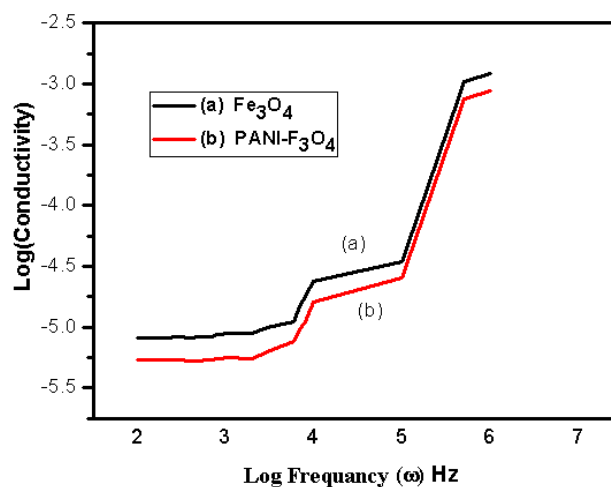


**Fig. 7:** Log conductivity of (a)  $\text{Fe}_3\text{O}_4$  and (b) PANI- $\text{Fe}_3\text{O}_4$  nanocomposite as a function of angular frequency.

AC-electrical conductivity was calculated using the equation:

$$\sigma_{a.c.}(\omega) = L/RA \quad (2)$$

Where: R is the electrical resistance (ohm), A is the surface area ( $\text{cm}^2$ ), L is the thickness (cm) and  $\omega$  is the angular frequency of the signal applied across the samples. AC-conductivities of as-prepared materials  $\text{Fe}_3\text{O}_4$  and PANI- $\text{Fe}_3\text{O}_4$  nanocomposite as a function of angular frequency is illustrated in Fig.7. In case of PANI- $\text{Fe}_3\text{O}_4$  nanocomposite, AC- conductivity increases with a rule of  $\sigma \propto \omega^n$  as it depends strongly on frequency. The value of the power exponent (n) can vary differently with the attitude of the conductivity at low and high frequency ranges of a transition region of M Hz. Other important characteristic behavior is that AC-conductivity increases low significantly at low and medium frequency, while it depends strongly at high frequency over 1 MHz. At medium frequency, some wavy characteristic behavior of the conductivity can be seen shifted to the higher frequency region. Other important property of electrical properties is the dielectric permittivity. The dielectric permittivity ( $\epsilon'$ ) of PANI- $\text{Fe}_3\text{O}_4$  nanocomposite were examined as a function of angular frequency (100Hz-5MHz) at room temperature and calculated using the following standard equation:

$$\epsilon' = \frac{C(F) \times d(m)}{\epsilon_0 \times A(m^2)} \quad (3)$$

Where  $\epsilon'$  is the real permittivity of the samples, d is the thickness (m), A is the surface area ( $\text{m}^2$ ), C is the capacitance (F) and  $\epsilon_0$  ( $= 8.852 \times 10^{-12}$  F/m) is the vacuum permittivity. As shown in Fig. 8, the permittivity with higher values observed at lower frequency region where the space charge polarization contribution is predominant (Elshafie et. al. 1999). The fast variation of the field accompanied with the applied frequency and electric dipoles are no longer able to rotate sufficiently fast to follow the field variation. This lead to a decrease in the value of permittivity with increasing of frequency (Field, and Chien, 1985).

It can be concluded that, Electrical properties of the nanocomposite studied; the dielectric properties and electrical conductivity in the frequency range 100Hz-5MHz. The conductivity of the nanocomposite linearly increases from  $1 \times 10^{-5}$  to  $1 \times 10^{-2}$  S/cm. The variation of conductivity with frequency reveals that the charge transport mechanism can be considered to be semiconductor. It is worthy to note from Fig. 8, that the measured and calculated permittivity decreases with increasing frequency. Also, it can be noticed that PANI- $\text{Fe}_3\text{O}_4$  nanocomposite has higher values of permittivity than  $\text{Fe}_3\text{O}_4$  overall the frequency range.

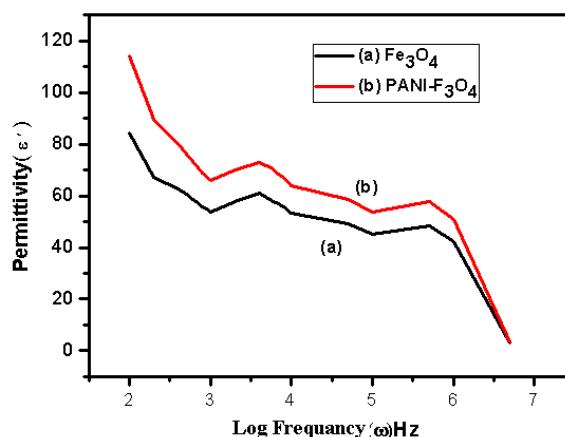


**Fig. 8:** Real Permittivity of (a) Fe<sub>3</sub>O<sub>4</sub>, and (b) PANI-Fe<sub>3</sub>O<sub>4</sub> nanocomposite as a function of angular frequency.

Semiconductors are the foundation of modern electronics, including radio, computers, and telephones. Semiconductor-based electronic components include transistors, solar cells, many kinds of diodes including the light-emitting diode (LED), the silicon controlled rectifier, photo-diodes, digital and analog integrated circuits. Increasing understanding of semiconductor materials and fabrication processes has made possible continuing increases in the complexity and speed of semiconductor devices. With controllable electrical, magnetic, and electromagnetic properties, the prepared nanocomposite may have potential applications in chemical sensors, catalysis, microwave absorbing, and electro-magneto-rheological fluids, etc..

#### Conclusions:

We have demonstrated a simple and reproducible one-pot synthesis of PANI nano particle containing Fe<sub>3</sub>O<sub>4</sub> NPs using APS as an oxidant via in situ self-assembly method to obtain the PANI-Fe<sub>3</sub>O<sub>4</sub> nanocomposite. The PANI-Fe<sub>3</sub>O<sub>4</sub> nanocomposite consists of long fibrils and granular particles. Electrical properties of the nanocomposite were studied measuring the electrical conductivity and dielectric properties in the frequency range 100Hz-5MHz at room temperature. The conductivity of the nanocomposite linearly increases from 1x10<sup>-5</sup> to 1x10<sup>-2</sup> S/cm. These values and the variation behavior of the conductivity with frequency reveals that the charge transport mechanism can be considered to be semiconductor. The prepared nanocomposite may have potential different applications.

#### References

- Alam, J., U. Riaz and S. Ahmad, 2007. Journal of Magnetism and Magnetic Materials, 314: 93-99.
- Alan, G., MacDiarmid, 2001. "Synthetic Metals": A Novel Role for Organic Polymers (Nobel Lecture)" Angew. Chem. Int. Ed., 40: 2581-2590. doi:10.1002/1521-3773(20010716)40:14
- Albuquerque, J.E., L.H.C. Mattoso, D.T. Balogh, R.M. Faria, J.G. Masters and A.G. MacDiarmid, 2000, Simple method to estimate the oxidation state of polyanilines, Synthetic Metals, 113(1/2): 19.
- Alexandre, M. and P. Dubois, 2000. Polymer-layered silicate nanocomposites: preparation, properties and uses of a new class of materials, Materials Science and Engineering: R: Reports, 28(1/2): 1.
- Amaya, T., Y. Nishina, D. Saio, and T. Hirao, 2008. Chem Lett., 37: 68-9.
- Aphesteguy, J.C. and S.E. Jacobo, 2004. Physica B 354: 224-227.
- Bai, H and G.Q. Shi, 2007. Gas sensors based on conducting polymers. Sensors., 7: 267-307.
- Bao, L. and J.S. Jiang, 2005. Physica B 367: 182-187.
- Berhard, W., 1994. Adv Mater., 6(3): 226- 8.
- Cao, Z., W. Jiang, X. Ye and X. Gong, 2008. Journal of Magnetism and Magnetic Materials, 320: 1499-1502.
- Chakrabarti, S., D. Ganguli and S. Chaudhuri, 2004. J. Phys., E24: 333-342.
- Chandrasekhar, P. and K. Naishadham, 1996. Synth. Met., 105: 115.
- Chen, Y., E.T. Kang, K.G. Neoh, S.L. Lim, Z.H. Ma and K.L. Tan, 2001 Intrinsic redox states of polyaniline studies by high-resolution X-ray photoelectron spectroscopy, Colloid and Polymer Science, 279(1) 73.
- Chiang, J.C. and A.G. MacDiarmid, 1986. Synth Met., 13: 193- 205.
- Deng, J.G., C.L. He, Y.X. Peng, J.H. Wang, X.P. Long, P. Li and A.S.C. Chan, 2003. Synth. Met.139, 295.
- Deng, J.G., X.B. Ding, W.H. Zhang, Y.X. Peng, J.H. Wang, X.P. Long, P. Li and A.S.C. Chan, 2002, Polymer, 43: 2179.



- Diaz, A.B., N.D.S. Mohallem and R.D. Sinisterra, 2004. Preparation of a Ferrofluid Using Cyclodextrin and Magnetite[J]. *J. Magn. Magn. Mater. R.*, 272: 2 395-2 397.
- Drelinkiewicz, A., A. Waksmundzka-Góra, J.W. Sobczak and J. Stejskal, 2007 *J. ApplCatal A*, 333: 219-28.
- Elsayed, A.H., M.S. Mohy Eldin, A.M. Elsyed, A.H. Abo Elazm, E.M. Younes and H.A. Motaweh, 2011. *Int. J. Electrochem. Sci.*, 6: 206-221.
- Elshafie, A., H.H. Afify and A. Abdel-All, 1999. *Phys. Stat. Sol.*, 174: 301.
- Feast, W.J. *et al.* 1996 Synthesis, processing and material properties of conjugated polymers, *Polymer*, 37(22): 5017-5047.
- Feng, B.Y., Su, J. Song and K. Kong, 2001. Electropolymerization of polyaniline/ montmorillonite nanocomposite, *Journal of Materials Science Letters*, 20(4): 293.
- Field, N.D. and M.C. Chien, 1985. *J. Appl. Polym. Sci.*, 30: 2103.
- Godovsky, D.Y., A.E. Varfolomeev, D.F. Zaretsky, C.R.L. Nayana, A. Kundig, C. Weder, *et al.* 2001. *J. Mater Chem.*, 11: 2465-9.
- Hua, C.C., S. Zakaria, R. Farahiyan, L.T. Khong, K.L. Nguyen, M. Abdullah and S. Ahmed, 2008. *SAINS Malays*, 37: 389-394.
- Huanga, Li-Ming, Cheng-Hou Chena and Ten-Chin Wen, 2006. Development and characterization of flexible electrochromic devices based on polyaniline and poly(3,4-ethylenedioxythiophene)-poly(styrene sulfonic acid) *Electrochimica Acta*; 51(26) : 5858-5863; (Article) doi:10.1016/j.electacta.2006.03.031
- Kazantseva, N.E., J. Vilcáková, V. Kresálek, P. Sába, I. Sapurina and J. Stejskal, 2004. Magnetic behaviour of composites containing polyaniline - coated manganese-zinc ferrite. *Journal of Magnetism and Magnetic Materials*, 269: 30-37.
- Kim, D.Y., J.Y. Lee, C.Y. Kim, E.T. Kang and K.L. Tan, 1995, Difference in doping behavior between polypyrrole films and powders, *Synthetic Metals.*, 72(3): 243.
- Klug, H.P. and L.E. Alexander, 1954. *X-Ray Diffraction Procedure*, Wiley Inter Science New York, pp: 504-524.
- Kryszewski, M. and J.K. Jeszka, 1998. *Synthetic Metals.*, 94: 99-104.
- Lankri, E., M.D. Levi, Y. Gofar, D. Aurbach and T. Otero, 2002. The behavior of polypyrrole- coated electrodes in propylene carbonate solutions. I. Characterization of PPy films by a combination of electroanalytical tools and XPS, *Journal of the Electrochemical Society*, 149(6): E 204.
- Li, L., J. Jiang and F. Xu, 2007. *Materials Letters*, 61: 1091-1096.
- Li, L., H. Liu, Y. Wang, J. Jiang and F. Xu, 2008. *Journal of Colloid and Interface Science* 321 , 265–271.
- MacDiarmid, A.G. and A.J., Epstein, 1995. *Synthetic Metals.*, 69: 86-92.
- Makeiff, D.A. and T. Huber, 2006 *Synth Met.*, 156: 497-505.
- Malinauskas, A. and R. Holze, 1999. In situ UV–vis spectroelectrochemical study of polyaniline degradation, *Journal of Applied Polymer Science*, 73(2): 287.
- Mathur, R., D.R. Sharma, S.R. Vadera and N. Kumar, 2001. *Acta mater.* 49: 181-187.
- Moghaddam, A.B. and T. Nazari, 2008. *Int. J. Electrochem. Sci.*, 3: 768-776.
- Pruneanu, S., E. Veress, I. Marian and L. Oniciu, 1999. Characterization of polyaniline by cyclic voltammetry and UV–vis absorption spectroscopy, *Journal of Materials Science*, 34(11): 2733.
- Rajagopalan, R. and J.O. Iroh, 2002. A one-step electrochemical synthesis of polyaniline– polypyrrole composite coatings on carbon fibers, *ElectrochimicaActa*, 47(12): 1847.
- Roselena, F., and M.M. Inacio, 2002. *J. Appl. Polym. Sci.*, 83: 1568.
- Sarac, A.S., M. Ates and B. Kilic, 2008. *Int. J. Electrochem. Sci.*, 3: 777-786.
- Shabnam, Virji, Jiaying Huang, Richard B. Kaner and Bruce H. Weiller, 2004. Polyaniline Nanofiber Gas Sensors: Examination of Response Mechanisms, *Nano Letters.*, 4(3): 491–496 (Article) doi:10.1021/nl035122e Abstract
- Soto-Oviedo, M.A., A.A. Faez, R.M.C. Rezende and M.A.D. Paoli, 2006, *Synth Met* ;156:1249-55.
- Stejskal J. and R G. Gilbert, 2002, *Pure Appl Chem.*, 74: 857-67.
- Sun, L.J., X.X. Liu, K.K.T. Lau, L.Chen and W.M. Gu, 2008. *Electrochim Acta.*, 53: 3036-42.
- Waldron RD 1955 Infrared spectra of ferrites. *Phys Rev.*, 99: 1727-1735.
- Wan, M.X., 1989. The influence of polymerization method and temperature on the absorption spectra and morphology of polyaniline. *Synth Met.*, 31: 51-59.
- Wan, M.X. and J.C. Li, 1999. *Synth. Met.*, 101: 844.
- Wan, M.X., W. Zhou and J.C. Li, 1996. *Synth. Met.*, 78: 27.
- Weng, C.J., Y.S. Jhuo, K.Y. Huang, C.F. Feng, J.M. Yeh and Y. Wei, *et al.* 2011. *Macromolecules.*, 44: 6067-76.
- Willner, I., B. Willner and E. Katz, 2007. *Bioelectrochemistry*, 70: 2-11.
- Yu, C., J. Zhai, Z. Li, M. Wan, M. Gao and L. Jiang, 2008. *Thin Solid Films*,
- Zhang, Z. and M. Wan, 2003. Nanostructures of polyaniline composites containing nano-magnet. *Synthetic Metals*, 132: 205-212.